SUPPLEMENTARY MATERIAL

LINDBLADIAN APPROACH TO M-PHOTON ABSORPTION

In this section, by drawing heavily on Refs. [1, 2], we provide details of the derivation of Lindbladian for mPA given in Eq. (4) of the main text. We assume that our sample consists of an ensemble of the systems that have two levels, i.e. $|1\rangle$ and $|2\rangle$. The transition of a two-level system takes place from state $|1\rangle$ to $|2\rangle$ by absorbing m photons simultaneously (see Fig. 1). We consider this m-photon transition resonant, hence $\omega_{12} = m\omega_0$. The interaction Hamiltonian is given by

$$H_I = \sum_i (\xi \sigma_{2i}^{\dagger} \sigma_{1i} E^{+m}(\vec{r}_i) + H.c.), \tag{A.1}$$

in which ξ is the matrix element for mPA, $\sigma_{1i}^{\dagger}$ and $\sigma_{2i}^{\dagger}$ are creation operators for ith two-level system in states of $|1\rangle$ and $|2\rangle$, respectively. The positive-frequency part of the electric field at the ith two-level system is given by

$$E^{+}(\vec{r}_i) = -i\sqrt{\frac{\hbar\omega}{2\epsilon_0}} u(\vec{r}_i) a, \tag{A.2}$$

where $u(\vec{r}_i)$ are the normalized mode eigenfunctions. The equation of motion for the density operator of the combined sample-photon field is

$$i\hbar \frac{\partial \rho_T(t)}{\partial t} = \left[\hat{H}_I', \rho_T(t)\right], \tag{A.3}$$

in which $\hat{H}_I'$ is the Hamiltonian in interaction picture. At $t = 0$, the two-level systems of the sample are decoupled from the photon field and

$$\rho_T(0) = \rho(0) \bigotimes \prod_i \rho(0)_i, \tag{A.4}$$

where $\rho(0)_i$ is the thermal-equilibrium density operator for the ith two-level system. The density operator of the photon-field at time t can be obtained by taking trace over two-level systems of the total density operator $\rho(t) = \mathrm{Tr}_i \rho_T(t)$. We can obtain the master equation by using the standard perturbation techniques based on Born-Markov approximations

$$\frac{\partial \rho(t)}{\partial t} = \frac{\kappa_1 \gamma_{mPA}}{2m}\left(\left[a^m \rho(t), a^{\dagger m}\right] + \left[a^m, \rho(t) a^{\dagger m}\right]\right) + \frac{\kappa_2 \gamma_{mPA}}{2m}\left(\left[a^{\dagger m} \rho(t), a^m\right] + \left[a^{\dagger m}, \rho(t) a^m\right]\right), \tag{A.5}$$

in which κ_1 (κ_2) is the thermal population of the two-level systems and γ_{mPA} is given by [1, 2]

$$\gamma_{mPA} = 2m\left(\frac{\hbar}{2\epsilon_0}\right)^{m-2} (2\pi)^2 \omega^m |\zeta|^2 g(m\omega) \int d^3 r N(\vec{r}) |u(\vec{r})|^{2m}, \tag{A.6}$$

in which $g(m\omega)$ is the line-shape function and $N(\vec{r})$ is the density of two-level systems at the position $\vec{r}$ and integration takes place over volume of the medium. The first term in Eq. (A.5) describes the absorption process while the second term accounts for the emission process. By considering the sample at zero temperature, ($\kappa_2 = 0$ and $\kappa_1 = 1$), (A.5) reduces to the Lindbladian in Eq. (4) of the main text.

HEISENBERG PICTURE CALCULATIONS

Here we describe how the optical signals and the measurement precision can be calculated straightforwardly in the Heisenberg picture. The squeezing operations in the two OPA's can be described by the following transformation on the photon annihilation operator [3]:

$$a \to a' = \cosh(r_k) a + \sinh(r_k) e^{i\phi_k} a^{\dagger}. \tag{A.7}$$

The imperfections in the experimental setups, i.e. single-photon losses, were modeled by beam splitter transformations. The beam splitter transformation approach to single-photon losses is well established for the description of imperfect photon detection or losses in the optical setup [4–6]. To describe scattering losses in the mPA medium rigorously, however, it would be

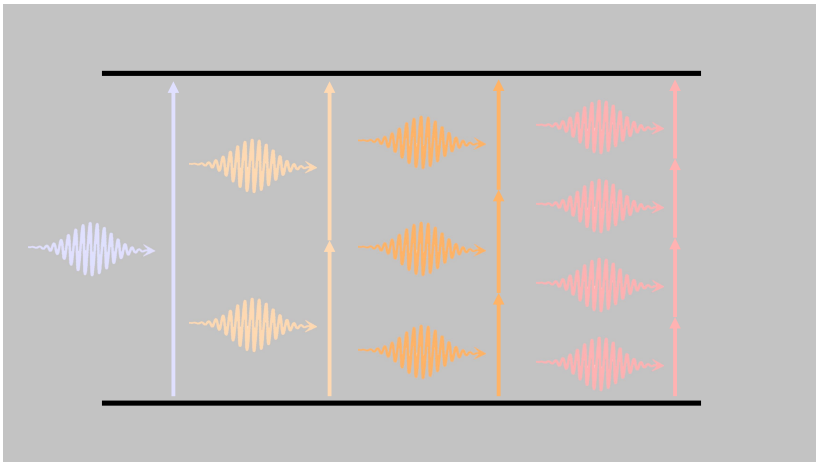

FIG. 1. Schematic presentation of the multiphoton absorption process considered in our study for a two-level system. Here, different colors correspond to different frequencies required for conducting one-, two-, three-, and four-photon absorption processes. It should be noted since we are dealing with the single mode in our study, each of these processes will take place by changing the frequency of the single mode, hence they will not happen simultaneously.

necessary to include them in the evolution equation (4) of the main text. This is not an issue for our analysis, as we evaluate the measurement precision in the limit $\varepsilon_m \ll 1$, but should be considered at finite absorbances. Modeling single-photon losses as unbalanced beam splitters, we obtain the input-output relation from Eq. (3) of the main text as [4–6]

$$a^{(out)} = \sqrt{\eta_k}\, a + \sqrt{1-\eta_k}\, c_k, \tag{A.8}$$

where c_k is the vacuum (empty port) photon annihilation operator. Using transformations in Eqs. (A.7) and (A.8), we can find the expectation value of the photon number in the following form:

$$\left.\frac{\partial\langle\hat{n}\rangle}{\partial\varepsilon}\right|_{\varepsilon=0} = \mathrm{tr}\left\{\hat{n}_f \rho_0\right\}, \tag{A.9}$$

in which

$$\hat{n}_f = U^\dagger_{loss\,2} U^\dagger_{OPA\,2} U^\dagger_{loss\,1} \mathcal{L}'^{\,adj}_{mPA}[U^\dagger_{OPA\,1}\hat{n}U_{OPA\,1}]U_{loss\,1}U_{OPA\,2}U_{loss\,2}, \tag{A.10}$$

where for a general operator X, $\mathcal{L}'^{\,adj}_{mPA}$ performs the following operation:

$$\mathcal{L}'^{\,adj}_{mPA}[X] = \frac{1}{2m}\left(2a'^{\,\dagger m} X a'^{m} - a'^{\,\dagger m} a'^{m} X - X a'^{\,\dagger m} a'^{m}\right), \tag{A.11}$$

and the corresponding operators in Eq. (A.10) are given by the transformations in Eqs. (A.12)-(A.17). The result for expectation value (A.9) is given in the Schrödinger picture. It is more convenient to perform the calculations in the Heisenberg picture. To do so, we introduce the following transformations in the Heisenberg picture for photons operators to evaluate Eq. (A.9):

1) We apply the displacement transformation which gives us

$$a \to a + |\alpha| e^{i\phi_{Las}}, \tag{A.12}$$

2) We apply the squeezing transformation (Eq. (A.7)) to account the first squeezing operation

$$a \to a' = \cosh(r_1)a + \sinh(r_1)a^\dagger, \tag{A.13}$$

in which, we have set $\phi_1 = 0$ without loss of generality.

3) Next, we apply the adjoint Lindbladian (A.11) to a'.

$$a' \to a'' = a' + \varepsilon_m \mathcal{L}^{adj}_{mPA}[a'] = a' - \frac{\varepsilon_m}{2} a'^{\dagger\, m-1} a'^{m}. \tag{A.14}$$

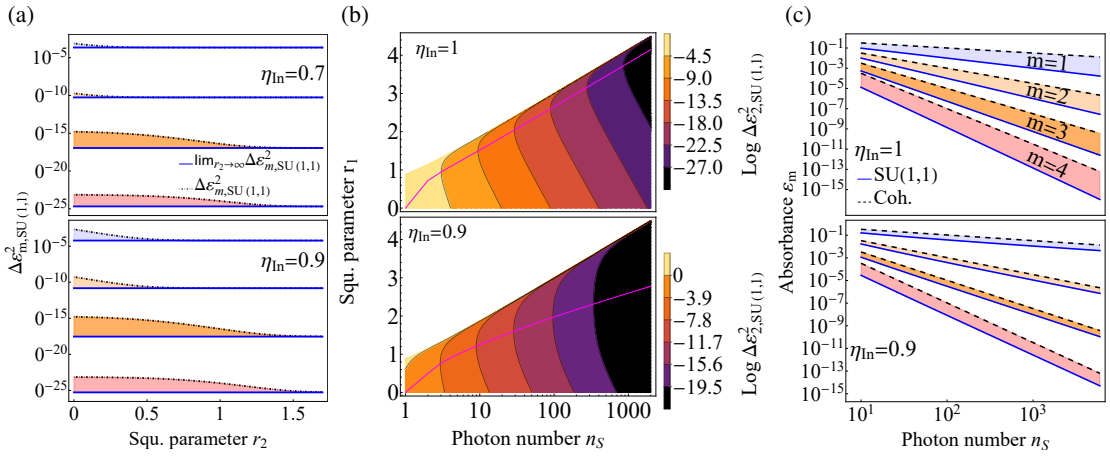

FIG. 2. (a) $\Delta\varepsilon^2_{2,SU(1,1)}$ (dotted-dashed lines) and Eq. (A.39) (solid lines) as a function of the second squeezing parameter for different internal losses. We observe that for a sufficiently large second squeezing parameter, $\Delta\varepsilon^2_{2,SU(1,1)}$ converges to Eq. (A.39). (b) Logarithm of $\Delta\varepsilon^2_{2,SU(1,1)}$ for a very large second squeezing parameter as a function of the first squeezing parameter and photon numbers. The magenta lines map the optimum regimes of the first squeezing parameter with their corresponding photon numbers. (c) The smallest absorbance that can be detected for a given photon number n_S^{min}, is shown for the optimal regime of sensitivity in the case of SU(1,1) and classical interferometers for one-, two-, three- and four-photon absorption processes. The absorbance is found by conditioning the signal-to-noise ratio (A.45) becoming one, i.e. $\varepsilon_m/\Delta\varepsilon_m = 1$.

4) For the internal loss, we perform the following transformation by using Eq. (A.8):

$$a'' \to a''_2 = \sqrt{\eta_{In}}a'' + \sqrt{1-\eta_{In}}c_1, \tag{A.15}$$

where for full justification on modeling single-photon loss by a beam splitter, please see appendix of Refs. [7] or Refs. [3, 4, 8].

5) We perform the squeezing operation with respect to the second OPA, which is described by the transformation $U^\dagger_{OPA\ 2}$ and Eq. (A.7):

$$a''_2 \to a''' = \cosh(r_2)a'' + e^{i\phi_{In}}\sinh(r_2)a''^\dagger. \tag{A.16}$$

6) Finally, to account for the external loss and by considering (A.8), we apply the following transformation:

$$a''' \to a'''_2 = \sqrt{\eta_{Ex}}a''' + \sqrt{1-\eta_{Ex}}c_2. \tag{A.17}$$

Finally, the expectation value of the transformed photon number operator $\hat{n}'' = a''^\dagger a''$ is taken with respect to the vacuum state, and the linear terms in ε_m are collected.

CALCULATION OF THE SCALING BEHAVIOR AT LARGE PHOTON NUMBERS

Here we derive Eqs. (6) and (7) of the main text. This derivation will also provide us with conditions on the necessary strength of the second squeezing parameter. To this end, we first note that from Eq. (A.11) we have

$$\mathcal{L}^{adj}_{mPA}[a''^\dagger a''] = -a''^{\dagger m}a''^m. \tag{A.18}$$

Coherent state transmission measurements

The variance of a coherent state with complex amplitude α is readily calculated as

$$\mathrm{Var}(\hat{n}) = |\alpha|^2 \tag{A.19}$$

From Eq. (A.18), we get the change of the photon number

$$\frac{\partial\langle\hat{n}\rangle}{\partial\varepsilon_m} = -|\alpha|^{2m}. \tag{A.20}$$

We next add internal and external losses, using the appropriate transformations above. In particular, the transformations (A.15) and (A.17) effectively yield the replacement $\alpha \to \eta_i\alpha$. Consequently, we find $\mathrm{Var}(\hat{n}) \to \eta_{In}\eta_{Ex}\mathrm{Var}(\hat{n})$ and $\partial\langle\hat{n}\rangle/\partial\varepsilon_m \to \eta_{In}\eta_{Ex}\partial\langle\hat{n}\rangle/\partial\varepsilon_m$. Altogether, we finally arrive at the result (6) of the main text.

Optimal states in SU(1,1) measurements

To find the photon number scaling of Eq. (5) of the main text, we first note that the second squeezing operation can be simplified in the limit of large r_2 to

$$\begin{aligned} a''' &= \cosh(r_2)a'' + e^{i\phi_{Int}}\sinh(r_2)a''^{\dagger} \\ &\simeq \frac{1}{2}e^{r_2}\left(a'' + e^{i\phi_{Int}}a''^{\dagger}\right) = \frac{e^{r_2+i\phi_{Int}/2}}{\sqrt{2}}\hat{q}_{\phi_{Int}/2}, \end{aligned} \tag{A.21}$$

where $\hat{q}_\phi = (a''e^{-i\phi} + a''^{\dagger}e^{i\phi})/\sqrt{2}$. With $\phi_{Int} = \pi$, this means the transformation turns any annihilation or creation operator into a momentum quadrature $\hat{p} = i(a^\dagger - a)/\sqrt{2}$ (modulo the prefactor) of the field at the sample. This can be seen in the variance of the photon number, which is given by

$$\mathrm{Var}(\hat{n}''') = \left(\frac{e^{2r_2}}{2}\right)^2\mathrm{Var}(\hat{p}''^2) + \left(\frac{e^{-2r_2}}{2}\right)^2\mathrm{Var}(\hat{q}''^2). \tag{A.22}$$

At sufficiently large r_2, the photon number variance of the light field at the detector is determined by the variance of the (squeezed) $\hat{p}$-quadrature at the sample,

$$\mathrm{Var}(\hat{n}''') = \left(\frac{e^{2r_2}}{2}\right)^2\mathrm{Var}(\hat{p}''^2). \tag{A.23}$$

To evaluate the latter, we write the operator as $\hat{p}'' = \Delta\hat{p} + \langle\hat{p}\rangle$. Here we have separated the expectation value (which grows with the photon number) from the squeezed fluctuation component $\Delta\hat{p} = \hat{p} - \langle\hat{p}\rangle$ with the properties $\langle\Delta\hat{p}\rangle = 0$ and $\langle\Delta\hat{p}^2\rangle = e^{-2r_1}/2$. This allows us to write

$$\begin{aligned} \mathrm{Var}(\hat{p}^2) &= \langle\hat{p}^4\rangle - \langle\hat{p}^2\rangle^2 \\ &= 4\langle\hat{p}\rangle^2\langle\Delta\hat{p}^2\rangle + \left(\langle\Delta\hat{p}^4\rangle - \langle\Delta\hat{p}^2\rangle^2\right). \end{aligned} \tag{A.24}$$

The second term in this equation is again exponentially small, $\langle\Delta\hat{p}^4\rangle - \langle\Delta\hat{p}^2\rangle^2 = e^{-4r_1}/2$. Consequently, the variance will be dominated by the first term, $4\langle\hat{p}\rangle^2\langle\Delta\hat{p}^2\rangle$, unless the expectation value of $\hat{p}$ becomes very small.

To continue, we note that we find *numerically* for the cases $m = 1,\ldots 4$ that the optimal states approximately fulfill $\langle\hat{p}\rangle^2 \simeq \langle\hat{q}^2\rangle = e^{2r_1}/2$. Furthermore, we note that for the amplitude-squeezed state with $\phi_{Las} = \pi/2$ the expectation value of the squeezed quadrature is given by $\langle\hat{p}\rangle = \sqrt{2}\alpha e^{-r_1}$, which implies the optimal amplitude is given by $\alpha = e^{2r_1}/2$, and we find that, altogether,

$$\mathrm{Var}(\hat{p}^2) \simeq 4\langle\hat{p}\rangle^2\langle\Delta\hat{p}^2\rangle = 1, \tag{A.25}$$

i.e. the variance of the optimal state remains constant for any photon number which is large enough to neglect the additional terms $\propto e^{-4r_1}$. Returning to Eq. (A.22), in order for the second term on the right-hand side of this equation to be negligible, the second squeezing parameter needs to be sufficiently large. We already established that $\mathrm{Var}(\hat{p}^2) \simeq 1$, and likewise find $\mathrm{Var}(\hat{q}''^2) \simeq e^{4r_1}/2$. With Eq. (A.22), this gives us

$$r_2 > \frac{r_1}{2} - \frac{1}{8}\log(2) \simeq \frac{r_1}{2}. \qquad \text{(Condition 1)} \tag{A.26}$$

With this result, we need to show that the denominator in Eq. (5) of the main text scales in the same way with the mean photon number as it did in the case of coherent states above, in order to prove the enhanced sensitivity scaling. To this end, we first note that for the optimal state, the mean photon number reads

$$\begin{aligned} \langle\hat{n}\rangle + \frac{1}{2} &= n_S + \frac{1}{2} = (\langle\hat{p}^2\rangle + \langle\hat{q}^2\rangle)/2 \simeq (\langle\hat{p}\rangle^2 + \langle\hat{q}^2\rangle)/2 \\ &\simeq \langle\hat{p}\rangle^2, \end{aligned} \tag{A.27}$$

where in the second line we used that $\langle\hat{q}^2\rangle = \langle\hat{p}\rangle^2$. Next, we combine Eqs. (A.14) and (A.16) to obtain

$$\frac{\partial\langle\hat{n}\rangle}{\partial\varepsilon_m} = \frac{e^{2r_2}}{2}\langle\mathcal{L}^{adj}_{mPA}[\hat{p}^2]\rangle \tag{A.28}$$

$$= \frac{e^{2r_2}}{2}\frac{1}{2}\left\langle\left(2\mathcal{L}^{adj}_{mPA}[a''^{\dagger}a''] - \mathcal{L}^{adj}_{mPA}[a''^2] - \mathcal{L}^{adj}_{mPA}[a''^{\dagger 2}]\right)\right\rangle \tag{A.29}$$

$$= \frac{e^{2r_2}}{4}\left\langle -2a''^{\dagger m}a''^m - \frac{m-1}{2}\left(a''^{\dagger m-2}a''^m + a''^{\dagger m}a''^{m-2}\right)\right\rangle. \tag{A.30}$$

If we assume for simplicity that these expectation values are dominated by the coherent amplitude (which for the optimal state is given by $\langle a\rangle = \sqrt{2}\langle\hat{p}\rangle$), we find that the first term in Eq. (A.30) scales as $\sim \langle\hat{p}\rangle^{2m}$, whereas the other terms account only for subdominant scaling $\sim \langle\hat{p}\rangle^{2m-2}$. Hence, with Eq. (A.27), this analysis shows that the denominator in Eq. (5) of the main text scales as n_S^m, just like in the measurement with coherent states analyzed above, but the variance (A.25) remains constant. Taken together, this proves the optimal photon number scaling of the mPA sensitivity, as described by Eq. (7) of the main text.

External losses change the momentum operator to $\hat{p} \to \sqrt{\eta_{Ex}}\hat{p} + \sqrt{1-\eta_{Ex}}\hat{p}_2$ (where $p_2 = i(c_2^{\dagger} - c_2)/\sqrt{2}$ is the corresponding quadrature of the auxiliary mode). As a consequence, the variance (A.23) becomes

$$\mathrm{Var}(\hat{n}''') \to \eta_{Ex}^2\left(\frac{e^{2r_2}}{2}\right)^2\mathrm{Var}(\hat{p}''^2) + \eta_{Ex}(1-\eta_{Ex})\frac{e^{2r_2}}{2}\left\langle\hat{p}^2\right\rangle. \tag{A.31}$$

The denominator of Eq. (5) of the main text simply becomes $\partial\langle\hat{n}\rangle/\partial\varepsilon_m = \eta_{Ex}e^{2r_2}\langle\mathcal{L}^{adj}_{mPA}[\hat{p}^2]\rangle/2$. Hence, if the first term in Eq. (A.31) is dominant, the external loss is compensated and we obtain the scaling behavior in Eq. 7 of the main text. This requirement gives us a bound on the value of the second squeezing parameter. Using Eqs. (A.25) and (A.27), we know that $\langle\hat{p}^2\rangle \simeq \langle\hat{p}\rangle^2 = e^{2r_1}/2$ and $\mathrm{Var}(\hat{p}''^2) \simeq 1$ which gives us

$$r_2 > r_1 + \log\left(\frac{1-\eta_{Ex}}{\eta_{Ex}}\right). \qquad \text{(Condition 2)} \tag{A.32}$$

For $\eta_{Ex} > 0.5$, the logarithmic term is negative and diverges to negative infinity as one approaches $\eta_{Ex} \to 1$. Hence, this condition is easily fulfilled when external losses are weak, such that Condition 1 determines the necessary squeezing parameter, but it becomes the relevant criterion in the presence of strong external losses.

Internal losses are not dealt with this easily. As we see numerically in Fig. 2 of the main text for $m = 1, \ldots 4$, these change the optimal scaling. We did not find a simple analytical result to describe this behavior.

Lindbladian approach to single-photon losses inside the sample

In this section, we consider the scenario that single-photon losses take place inside the sample simultaneously with the weak mPA process, such that the time evolution of the propagating light field inside the sample is given by

$$\frac{d}{dt}\rho = (\gamma_{mPA}\mathcal{L}_{mPA} + \gamma_{SPA}\mathcal{L}_{SPA})\,\rho, \tag{A.33}$$

in which the first term accounts for mPA losses [see Eq. (4) of the main text], γ_{SPA} is the single-photon loss coefficient, and $\mathcal{L}_{SPA}$ describes single-photon loss inside the sample via the following Lindbladian

$$\mathcal{L}_{SPA}\rho = \left(2a\rho a^{\dagger} - a^{\dagger}a\rho - \rho a^{\dagger}a\right). \tag{A.34}$$

The solution to Eq. (A.33) can be found straightforwardly as

$$\rho(t) = \exp\left(\mathcal{L}_{TPA}\varepsilon_m + \mathcal{L}_{SPA}\varepsilon_s\right)\rho_0, \tag{A.35}$$

in which $\varepsilon_s = \gamma_{SPA} \times t$. In our study, we investigated mPA perturbatively. The same can not be done for single-photon loss inside the sample as this process could be much larger. Considering that $\mathcal{L}_{mPA}$ and $\mathcal{L}_{SPA}$ do not commute, to evaluate the numerator and denominator of Eq. (5) of the main text, we use the Suzuki-Trotter resulting in (see [7])

$$\frac{\partial}{\partial\varepsilon_m}\exp\left(\mathcal{L}_{mPA}\varepsilon_m + \mathcal{L}_{SPA}\varepsilon_s\right) \tag{A.36}$$

$$= \int_0^1 dk\ \exp[(1-k)\mathcal{L}_{SPA}\varepsilon_s]\mathcal{L}_{mPA}\exp[k\mathcal{L}_{SPA}\varepsilon_s], \tag{A.37}$$

which indicates that the single-photon loss inside the sample can be described by a convolution of losses taking place before and after the mPA event. We can use the beam splitter approach to model these losses with $\eta_{before} = \exp(-2k\varepsilon_s)$ and $\eta_{after} = \exp(-2(1-k)\varepsilon_s)$ followed by a simple integral over k, and the total single-photon loss is given by $\eta_{In} = \eta_{before}\eta_{after} = \exp(-2\varepsilon_s)$. This means that before the mPA transformation in Eq. (A.14), one should insert a beam splitter transformation $a' \to \sqrt{\eta_{before}}a' + \sqrt{1-\eta_{before}}c_0$ to account for the single photon losses before the sample. The single-photon loss after the sample can be included into η_{In} as it is pointed out before. Using the additional transformation for photon loss before the sample, one can find the variance and denominators of Eq. 5 of the main text and take the integral with respect to k. Finding a closed expression analogous to Eq. (A.18) for the output field is difficult for general m and arbitrary input states. However, we find the following behavior for coherent state measurements with $2 \leq m \leq 4$

$$\Delta\varepsilon^2_{m,(coh)} = \frac{(m-1)^2\log^2(\eta_{In})}{(1-\eta_{In}^{m-1})^2}\frac{1}{\eta_{In}\eta_{Ex}n_S^{2m-1}}, \tag{A.38}$$

Comparing (A.38) with (6) of the main text, we notice that the first term in Eq. (A.38) originates from the single-photon loss inside the sample which can highly degrade $\Delta\varepsilon^2_{m,(coh)}$. The full solution of the squeezed coherent state contains many different terms [see our previous discussion following Eq. (A.21)], in general. If we only consider the change of the leading order in n_s from Eq. (A.30), we obtain a similar prefactor as for the coherent state.

Final expressions in the imbalanced regime

Having establishing the feasibility of obtaining $\Delta\varepsilon^2_{m,SU(1,1)}$ in the limit of the large second squeezing parameter ($r_2 \to \infty$), here we provide the explicit expressions for the variance $\Delta\varepsilon^2_{m,SU(1,1)}$ in this limit for one-, two-, three- and four-photon absorption processes, which we used to produce the plots in the manuscript. Explicitly, we find

$$\Delta\varepsilon^2_{m,SU(1,1)}\Big|_{r_2\to\infty} = \frac{A}{\eta_{In}^2 A_m}, \tag{A.39}$$

where

$$A = 8\eta_{In}\left(2\alpha^2 + 2\left(8\alpha^2+1\right)\eta_{In}n_{\mathrm{r1}}^2(1-\sqrt{n_{\mathrm{r1}}^2+n_{\mathrm{r1}}}) - \left(4\alpha^2\eta_{In}+4\alpha^2+1\right)\sqrt{n_{\mathrm{r1}}^2+n_{\mathrm{r1}}} + \left(\left(12\alpha^2+1\right)\eta_{In}+4\alpha^2+1\right)n_{\mathrm{r1}}\right)+2, \tag{A.40}$$

$$A_1 = \left(4\alpha^2+1\right)^2\left(2n_{\mathrm{r1}} - 2\sqrt{n_{\mathrm{r1}}^2+n_{\mathrm{r1}}}+1\right)^2, \tag{A.41}$$

$$A_2 = \left[\left(4\alpha^2+3\right)\alpha^2 + \left(32\alpha^4+48\alpha^2+6\right)\left[n_{\mathrm{r1}}^2 - \sqrt{n_{\mathrm{r1}}^4+n_{\mathrm{r1}}^3}\right] + 4\left(8\alpha^4+10\alpha^2+1\right)n_{\mathrm{r1}} - \left(16\left(\alpha^4+\alpha^2\right)+1\right)\sqrt{n_{\mathrm{r1}}^2+n_{\mathrm{r1}}}\right]^2, \tag{A.42}$$

$$\begin{aligned} A_3 = \Big[&\left(4\alpha^2+5\right)\alpha^4 - 2\left(12\alpha^4+23\alpha^2+6\right)\alpha^2\sqrt{n_{\mathrm{r1}}^2+n_{\mathrm{r1}}} + 3\left(4\alpha^2+3\right)\left(16\alpha^4+40\alpha^2+3\right)n_{\mathrm{r1}}^2 + \left(72\alpha^6+178\alpha^4+78\alpha^2+3\right)n_{\mathrm{r1}} \\ &+ 2\left(64\alpha^6+240\alpha^4+180\alpha^2+15\right)\left[n_{\mathrm{r1}}^3 - \sqrt{n_{\mathrm{r1}}^6+n_{\mathrm{r1}}^5}\right] - 4\left(32\alpha^6+96\alpha^4+54\alpha^2+3\right)\sqrt{n_{\mathrm{r1}}^4+n_{\mathrm{r1}}^3}\Big]^2, \end{aligned} \tag{A.43}$$

$$\begin{aligned} A_4 = \Big[&\left(4\alpha^2+7\right)\alpha^6 - \left(32\alpha^4+92\alpha^2+45\right)\alpha^4\sqrt{n_{\mathrm{r1}}^2+n_{\mathrm{r1}}} + \left(128\alpha^6+488\alpha^4+414\alpha^2+63\right)\alpha^2 n_{\mathrm{r1}} + \\ &2\left(256\alpha^8+1792\alpha^6+3360\alpha^4+1680\alpha^2+105\right)\left[n_{\mathrm{r1}}^4 - \sqrt{n_{\mathrm{r1}}^8+n_{\mathrm{r1}}^7}\right] + \\ &\left(640\alpha^8+3352\alpha^6+4458\alpha^4+1467\alpha^2+54\right)n_{\mathrm{r1}}^2 + 16\left(64\alpha^8+400\alpha^6+660\alpha^4+285\alpha^2+15\right)n_{\mathrm{r1}}^3 - \\ &3\left(256\alpha^8+1536\alpha^6+2400\alpha^4+960\alpha^2+45\right)\sqrt{n_{\mathrm{r1}}^6+n_{\mathrm{r1}}^5} - \left(320\alpha^8+1496\alpha^6+1698\alpha^4+432\alpha^2+9\right)\sqrt{n_{\mathrm{r1}}^4+n_{\mathrm{r1}}^3}\Big]^2, \end{aligned} \tag{A.44}$$

in which for the sake brevity, we have used $\sinh^2(r_1) = n_1$.

Evidently, these expressions are independent of external loss. While we are using the above formulas to conduct our study, it should be noted that the threshold for $\Delta\varepsilon^2_{2,SU(1,1)}$ converging to $\Delta\varepsilon^2_{2,SU(1,1)}\Big|_{r_2\to\infty}$ can be reached with realistic squeezing strengths. In panel (a) of Fig. 2 (and panel c of Fig. 1 in main text), we show numerically how the variance (5) converges to the $r_2 \to \infty$-limit with increasing second squeezing parameter for different internal losses and photon number at the sample n_S. The convergence between $\Delta\varepsilon^2_{m,SU(1,1)}$ and $\Delta\varepsilon^2_{m,SU(1,1)}\Big|_{r_2\to\infty}$ is dictated by three factors - the mean photon number, internal loss, and the degree of the nonlinearity. This regime of convergence for the second squeezing parameter can be experimentally realized and it is to this converging behavior that allows us to use Eqs. A.40-A.44 to investigate the enhancement in SU(1,1) interferometers in the high-gain regime of $r_2 \to \infty$.

Using the limit $r_2 \to \infty$ (Eqs. A.40-A.44), the next step is finding the optimum sensitivity by optimizing the first squeezing parameter for different internal loss and incident photon numbers. In panel (b) of Fig. 2, we have done so for a two-photon absorption process in the case of different internal losses ($\eta_{In} = 1$ and 0.9). The white area in these diagrams corresponds to nonphysical parameters, where $\sinh^2(r_1) > n_S$. The borderline between the white area and contour plots is the (unseeded) squeezed vacuum case, i.e. $r_1 = \text{arcsinh}\sqrt{n_S}$ and $\alpha = 0$. Within the allowed region for the first squeezing parameter, there is a unique optimal first squeezing parameter at each incident photon number and internal loss. This unique first squeezing parameter is an increasing function of the incident photon number and a decreasing function of the internal loss. In the absence of internal losses, we find that it satisfies approximately $\langle\hat{p}\rangle^2 = \langle\hat{q}^2\rangle$, as we used in our derivation above.

We can use the obtained optimal regime of the first squeezing parameter to investigate the minimal number of photons n_S^{min} necessary to observe a signal. This minimal photon number is where the signal-to-noise ratio (SNR)

$$SNR = \varepsilon_m \frac{\left|\frac{\partial\langle\hat{n}\rangle}{\partial\varepsilon_m}\right|}{\sqrt{\text{Var}\,(\hat{n})}} = \frac{\varepsilon_m}{\Delta\varepsilon_m}, \tag{A.45}$$

becomes one, i.e. the signal becomes as large as the noise. In panel (c) of Fig. 2, we have plotted absorbance as a function of the minimal photon number for SU(1,1) interferometer and classical measurements with different degrees of mPA and internal loss. In an ideal case, the unit SNR would be achieved at a considerably smaller photon number in an SU(1,1) interferometer compared to its classical counterpart for the same absorbance. Although the enhancement offered by interferometric detection can be negatively affected by internal loss, even in the presence of strong internal loss, our strategy still outperforms any classical measurement. It should be noted that external loss would degrade the results for the conditioned SNR of the classical strategy even further whereas our strategy in SU(1,1) interferometer is independent of external loss.

THE RELATION TO ABSORPTION CROSS SECTIONS AND ESTIMATE OF THEIR MAGNITUDE

Here we discuss the relation between the absorbance ε_m and experimentally measured absorption cross sections.

To this end, we first turn to the measurement of two-photon cross sections and make the connection to the measurement of TPA with squeezed vacuum, in particular. The measurement is typically related to the change of the photon count rate ΔR_2 with and without the sample inserted in the beam. Taking a squeezed vacuum input state, this change is then related to the photon flux density ϕ as

$$\Delta R_2 = \nu(\sigma_e\phi + \delta_r\phi^2). \tag{A.46}$$

Here, we have used the conventional nomenclature, where σ_e (in units m^2) denotes the entangled absorption cross-section stemming from photon pairs that are generated in the same downconversion event. δ_r ($m^4 s$) is the classical two-photon absorption cross-section, and the corresponding change of the photon count rate scales quadratically with the photon flux density.

We next follow the arguments by Parzuchowski et al. [9], and relate the photon flux density to the mean photon number of a single mode state (per pulse) as

$$\phi = \frac{\langle\hat{n}\rangle}{TA}, \tag{A.47}$$

where we define the pulse duration T and the beam area A. We calculate the change of the photon number using the formalism presented in the previous sections. For a squeezed vacuum, this yields in the absence of single-photon losses $\partial\langle\hat{n}\rangle/\partial\varepsilon_2 = n_0 + 3n_0^2$ [7], where $n_0 = \sinh^2(r)$ is the mean photon number of the pulse (For a coherent state with complex amplitude α, we would likewise obtain $\partial\langle\hat{n}\rangle/\partial\varepsilon_2 = n_\alpha^2$ with mean photon number $n_\alpha = |\alpha|^2$). We further assume that two-photon absorption takes place in a sample with density ν and volume $V = A\ell$, where ℓ is the sample length. We can then identify the change of the photon

count rate as $\Delta R_2 = \varepsilon_2 \partial\langle\hat{n}\rangle/\partial\varepsilon_2 T^{-1}$, assuming that the photon flux across the full beam area A is detected. Taken together, we can use these relations to turn the absorbance into a cross-section by writing

$$\varepsilon_2 = \sigma_e \nu \ell. \tag{A.48}$$

Likewise, we can connect the entangled cross-section to the classical counterpart as

$$\delta_r = 3\sigma_e T A, \tag{A.49}$$

i.e. the classical two-absorption cross section will in general depend on the experimental parameters.

We next provide an estimate for the absorbance one could expect in an experiment. We use parameters from Ref. [10] for a two-photon absorption measurement in rhodamine B molecules, $\sigma_e = 4.2\times10^{-18}$ cm^2 / molecule and a concentration of 38 μM. Assuming further a reasonable length of a cuvette of $\ell = 1$ mm, we end up with $\varepsilon_2 \simeq 10^{-2}$. We remark that the values of entangled two-photon absorption cross sections vary strongly in the literature (for a review of the debate, see e.g. [11]), and we employed one of the largest reported cross sections in our estimate. Hence, $\varepsilon_2 \simeq 10^{-2}$ should perhaps be considered an upper bound for realistic absorbances.

To the best of our knowledge, multi-photon absorption of squeezed light has not been reported beyond $m = 2$ to date. However, we can obtain a rough estimate for ε_m by noting that in semiclassical light-matter interactions, the m-photon absorption rate is related to the $2m-1$-th nonlinear susceptibility [12]. Its strength can be estimated according to the argument provided in Boyd's book [13] relating the nonlinear susceptibility to the characteristic atomic field strength $E_{at} = 5.14\times10^{11}$ V / m. Thus, we have $\chi^{(n)} \sim \chi^{(1)}/E_{at}^{n-1}$, where the linear susceptibility $\chi^{(1)} = O(1)$ is the linear susceptibility. Counteracting this steep decrease, we can expect an enhancement of nonlinear light-matter interactions due to the photon statistics of the light fields related to its normally ordered, normalized correlation function $g^{(m)}$ and the m-th power of the photon number, $\langle\hat{n}\rangle^m$ [1, 14], which for the case of squeezed vacuum increases as a double-factorial $\sim (2m-1)!!$ [15]. We, therefore, end up with

$$\varepsilon_m \sim (2m-1)!! \times \langle\hat{n}\rangle^m / E_{at}^{2m-2}. \tag{A.50}$$

This scaling behavior does not enable us to obtain explicit estimates for ε_m, but as long as the involved field intensities (corresponding to $\langle\hat{n}\rangle$) are much smaller than E_{at}^2, i.e. as long as the light-matter interaction can be treated perturbatively, they can be expected to decrease rapidly with m.

[1] G. S. Agarwal, Field-correlation effects in multiphoton absorption processes, Phys. Rev. A **1**, 1445 (1970).
[2] M. S. Zubairy and J. J. Yeh, Photon statistics in multiphoton absorption and emission processes, Phys. Rev. A **21**, 1624 (1980).
[3] S. Barnett and P. Radmore, *Methods in Theoretical Quantum Optics* (Oxford University Press, 2002).
[4] P. D. Drummond and Z. Ficek, *Quantum Squeezing* (Springer Berlin, Heidelberg, 2004).
[5] M. Manceau, G. Leuchs, F. Khalili, and M. Chekhova, Detection loss tolerant supersensitive phase measurement with an su(1,1) interferometer, Phys. Rev. Lett. **119**, 223604 (2017).
[6] M. Manceau, F. Khalili, and M. Chekhova, Improving the phase super-sensitivity of squeezing-assisted interferometers by squeeze factor unbalancing, New Journal of Physics **19**, 013014 (2017).
[7] S. Panahiyan, C. S. Muñoz, M. V. Chekhova, and F. Schlawin, Two-photon-absorption measurements in the presence of single-photon losses, Phys. Rev. A **106**, 043706 (2022).
[8] C. Gardiner and P. Zoller, *Quantum Noise* (Springer Berlin, Heidelberg, 2004).
[9] K. M. Parzuchowski, A. Mikhaylov, M. D. Mazurek, R. N. Wilson, D. J. Lum, T. Gerrits, C. H. Camp, M. J. Stevens, and R. Jimenez, Setting bounds on entangled two-photon absorption cross sections in common fluorophores, Phys. Rev. Applied **15**, 044012 (2021).
[10] J. P. Villabona-Monsalve, O. Calderón-Losada, M. Nuñez Portela, and A. Valencia, Entangled two photon absorption cross section on the 808 nm region for the common dyes zinc tetraphenylporphyrin and rhodamine b, The Journal of Physical Chemistry A **121**, 7869 (2017).
[11] B. P. Hickam, M. He, N. Harper, S. Szoke, and S. K. Cushing, Single-photon scattering can account for the discrepancies among entangled two-photon measurement techniques, The Journal of Physical Chemistry Letters **13**, 4934 (2022).
[12] P. Cronstrand, Y. Luo, and H. Ågren, Multi-photon absorption of molecules, in *Advances in Quantum Chemistry*, Response Theory and Molecular Properties (A Tribute to Jan Linderberg and Poul Jørgensen), Vol. 50 (Academic Press, 2005) pp. 1–21.
[13] R. W. Boyd, *Nonlinear Optics, Third Edition*, 3rd ed. (Academic Press, Inc., USA, 2008).
[14] B. R. Mollow, Two-photon absorption and field correlation functions, Phys. Rev. **175**, 1555 (1968).
[15] K. Y. Spasibko, D. A. Kopylov, V. L. Krutyanskiy, T. V. Murzina, G. Leuchs, and M. V. Chekhova, Multiphoton effects enhanced due to ultrafast photon-number fluctuations, Phys. Rev. Lett. **119**, 223603 (2017).